RESEARCH PAPER

DEVELOPMENT AND OPTIMIZATION OF ANTICANCER DRUG NANOCRYSTALS USING A QUALITY BY DESIGN APPROACH TO IMPROVE SOLUBILITY AND DISSOLUTION PERFORMANCE

Anita G. Rathod[1*], Dr. Narendra Silawate[2]
[1*]Research Scholar, Department of Pharmacy, Oriental University, Indore (M.P)-453555
[2]Supervisor, Department of Pharmacy, Oriental University, Indore (M.P)-453555
Corresponding Author,
Anita G. Rathod,
Research Scholar,
Department of Pharmacy,
Oriental University, Indore (M.P)-453555
Email ID: anitarathod812@gmail.com
Received: 12 th May, 2026; Revised: 17 th June, 2026; Accepted: 10 th July, 2026; Available Online: 15 th July, 2026

ABSTRACT:
Background: Cisplatin is a widely used platinum-based anticancer agent; however, its clinical performance is limited by poor aqueous solubility and low permeability, resulting in reduced dissolution and biopharmaceutical performance. Nanocrystal technology has emerged as an effective strategy to overcome these limitations by enhancing the dissolution characteristics of poorly soluble drugs.
Objective: The present study aimed to develop and optimize cisplatin nanocrystals using a Quality by Design (QbD) approach to improve their physicochemical properties, dissolution performance, and formulation stability.
Methods: Cisplatin nanocrystals were prepared using the anti-solvent precipitation technique followed by high-pressure homogenization. A Box–Behnken experimental design was employed to optimize the formulation variables, including drug concentration, stabilizer concentration, homogenization pressure, and homogenization cycles. The optimized formulation was characterized for particle size, polydispersity index (PDI), zeta potential, crystallinity (XRD), thermal behavior (DSC and TGA), drug content, encapsulation efficiency, and HPLC analysis. Statistical optimization was performed using response surface methodology.
Results: The optimized nanocrystals exhibited a mean particle size of approximately 160 nm, a PDI of 0.21, and a zeta potential ranging from −45 to −50 mV, indicating a stable and homogeneous nanosuspension. XRD and DSC analyses demonstrated reduced crystallinity following nanosization, while TGA confirmed adequate thermal stability. The optimized formulation achieved a drug content of 98.2 ± 1.1% and an encapsulation efficiency of 89.7 ± 1.4%. The validated HPLC method showed excellent linearity, precision, and accuracy for quantitative drug estimation. Overall, the optimized formulation exhibited superior physicochemical characteristics compared with the pure drug.
Conclusion: The QbD-based formulation strategy successfully produced stable cisplatin nanocrystals with reduced particle size, improved solid-state characteristics, and high drug incorporation efficiency. These findings demonstrate the potential of nanocrystal technology as an effective platform for enhancing the pharmaceutical performance of poorly soluble BCS Class IV anticancer drugs and provide a robust foundation for subsequent dissolution, permeability, and biological evaluation studies.
Keywords: Cisplatin**,** Nanocrystals**,** Quality by Design (QbD)**,** Anti, solvent Precipitation**,** High-Pressure Homogenization**,** Particle Size**,** Dissolution Enhancement**,** Drug Delivery**,** BCS Class IV Drug.
How to cite this article: Anita G. Rathod1* Dr. Narendra Silawate2. DEVELOPMENT AND OPTIMIZATION OF ANTICANCER DRUG NANOCRYSTALS USING A QUALITY BY DESIGN APPROACH TO IMPROVE SOLUBILITY AND DISSOLUTION PERFORMANCE. Int J Drug Deliv Technol. 2026;16(76s):2296-2310. DOI: 10.25258/ijddt.16.76s.230

.INTRODUCTION:

Cancer remains one of the leading causes of morbidity and mortality worldwide, accounting for millions of new cases and deaths annually. Despite significant advances in diagnosis and therapeutic strategies, chemotherapy continues to play a pivotal role in the management of both solid and hematological malignancies.[1] Among the available chemotherapeutic agents, platinum-based compounds have remained the cornerstone of cancer treatment because of their broad-spectrum antitumor activity and proven clinical efficacy against ovarian, testicular, lung, bladder, head and neck, and several other malignancies.[2-4] Their therapeutic action primarily involves the formation of DNA cross-links, resulting in inhibition of DNA replication and transcription, ultimately inducing apoptosis in rapidly proliferating cancer cells. However, the clinical performance of many platinum-based anticancer drugs is often restricted

by unfavorable physicochemical and biopharmaceutical properties, which limit their therapeutic efficiency.[5-7]

One of the major challenges associated with several anticancer agents is their poor aqueous solubility and limited membrane permeability, leading to inadequate dissolution, variable absorption, and suboptimal drug delivery. These limitations frequently necessitate the administration of higher doses to achieve therapeutic plasma concentrations, which consequently increases the risk of systemic toxicity and adverse effects. In addition, poor dissolution behavior may reduce drug availability at the target site, thereby compromising treatment efficacy. Improving the dissolution characteristics and bioavailability of poorly soluble anticancer drugs has therefore become an important objective in modern pharmaceutical formulation research.[8-10]

Several formulation strategies have been investigated to overcome the limitations associated with poorly soluble drugs, including solid dispersions, liposomes, polymeric nanoparticles, micelles, nanoemulsions, self-emulsifying drug delivery systems, cyclodextrin inclusion complexes, and lipid-based carriers. Although these technologies have demonstrated varying degrees of success, they often require complex manufacturing procedures, specialized excipients, relatively low drug loading, or involve challenges related to stability, scalability, and regulatory acceptance.[11-14] Consequently, there remains a continuous need for formulation approaches that are simple, scalable, cost-effective, and capable of improving drug dissolution without altering the chemical structure of the active pharmaceutical ingredient.

Nanocrystal technology has emerged as one of the most promising formulation approaches for enhancing the performance of poorly water-soluble drugs. Pharmaceutical nanocrystals are pure drug particles generally ranging from 100 to 1000 nm, stabilized by suitable surfactants or polymers to prevent particle aggregation. Unlike carrier-based nanoparticulate systems, nanocrystals consist predominantly of the active pharmaceutical ingredient, allowing high drug loading while minimizing the use of additional excipients. The significant reduction in particle size results in a substantial increase in surface area, saturation solubility, and dissolution rate according to the Noyes–Whitney and Ostwald–Freundlich principles. These improvements can ultimately enhance drug absorption, therapeutic efficacy, and dose uniformity.[15-17]

Nanocrystal formulations offer several additional advantages over conventional delivery systems. Their relatively simple composition facilitates large-scale manufacturing using established pharmaceutical processes such as wet milling, high-pressure homogenization, and anti-solvent precipitation. Furthermore, nanocrystals exhibit excellent versatility and can be incorporated into multiple dosage forms, including oral tablets, capsules, injectables, topical formulations, and implantable systems. Numerous commercially available pharmaceutical products based on nanocrystal technology have demonstrated improved dissolution characteristics, enhanced bioavailability, and better patient outcomes, highlighting the clinical relevance of this formulation strategy.[18-20]

Among the available manufacturing techniques, anti-solvent precipitation followed by high-pressure homogenization has attracted considerable attention because of its simplicity, reproducibility, and scalability. During anti-solvent precipitation, rapid supersaturation promotes instantaneous nucleation and formation of fine drug particles, while subsequent high-pressure homogenization effectively reduces particle size and narrows the particle size distribution. Appropriate selection of stabilizers is essential to maintain colloidal stability by preventing crystal growth and particle aggregation throughout the preparation process. The optimization of formulation variables such as stabilizer concentration, homogenization pressure, and processing cycles is therefore critical for obtaining nanocrystals with desirable physicochemical characteristics and long-term stability.[21]

Quality by Design (QbD) has become an integral component of contemporary pharmaceutical development because it emphasizes systematic process understanding and scientific optimization rather than empirical trial-and-error experimentation. QbD involves identifying critical material attributes and critical process parameters that influence the critical quality attributes of the final product. Statistical experimental designs, particularly the Box–Behnken Design (BBD), enable efficient evaluation of formulation variables and their interactions while minimizing the number of experimental runs. Response Surface Methodology further facilitates optimization by establishing mathematical relationships between formulation variables and product responses, thereby improving process robustness, reproducibility, and regulatory compliance.[22-24]

The successful development of nanocrystal formulations requires comprehensive physicochemical characterization to ensure product quality and stability. Parameters such as particle size, polydispersity index, zeta potential, crystallinity, thermal behavior, drug content, encapsulation efficiency, and analytical method validation provide valuable information regarding formulation performance and stability. Techniques including dynamic light scattering (DLS), Fourier transform infrared spectroscopy (FTIR), X-ray diffraction (XRD), differential scanning calorimetry (DSC), thermogravimetric analysis

(TGA), and high-performance liquid chromatography (HPLC) are routinely employed to evaluate these critical quality attributes and confirm the successful preparation of nanocrystals.

Based on these considerations, the present study was undertaken to develop and optimize an anticancer drug nanocrystal formulation using a Quality by Design (QbD) approach. Nanocrystals were prepared by anti-solvent precipitation followed by high-pressure homogenization, and formulation variables were optimized using a Box–Behnken Design. The optimized formulation was comprehensively characterized with respect to particle size, polydispersity index, zeta potential, crystallinity, thermal behavior, drug content, encapsulation efficiency, and chromatographic performance. The study aimed to establish a robust and reproducible formulation strategy capable of improving the physicochemical properties and dissolution performance of poorly soluble anticancer drugs, thereby providing a promising platform for enhanced pharmaceutical and therapeutic applications.

MATERIALS AND METHODS:

MATERIALS:

Cisplatin (purity ≥99%) was obtained as a gift sample from by Balaji Drugs Pvt. Ltd., Surat, Gujarat, India. Polyvinylpyrrolidone K30 (PVP K30), Hydroxypropyl Methylcellulose (HPMC), Poloxamer 188, Tween 80, ethanol, methanol, and potassium bromide (KBr) were purchased from HiMedia Laboratories Pvt. Ltd., Mumbai, India. Distilled water was prepared in-house and used throughout the study. Certified reference standards for differential scanning calorimetry (DSC) and gold–palladium sputtering targets for scanning electron microscopy (SEM) were procured from standard commercial suppliers. All chemicals and reagents used were of analytical reagent (AR) grade and were used without further purification.

METHOD:

Preformulation Studies

Comprehensive preformulation studies were conducted to investigate the physicochemical characteristics of cisplatin and to assess its compatibility with the selected pharmaceutical excipients prior to nanocrystal development. The organoleptic properties, aqueous solubility, partition coefficient (log P), melting point, and spectral characteristics of the drug were evaluated using standard analytical procedures. Drug–excipient compatibility studies were performed using FTIR spectroscopy and DSC by analyzing physical mixtures of cisplatin with Polyvinylpyrrolidone K30 (PVP K30), Hydroxypropyl Methylcellulose (HPMC), Poloxamer 188, and Tween 80. In addition, preliminary solubility enhancement studies were conducted to identify suitable stabilizers for nanocrystal formulation.[25-27]

Solubility Determination

The equilibrium solubility of cisplatin was determined using the shake-flask method. An excess amount of drug was added to 5 mL of distilled water, phosphate buffer solutions (pH 1.2, 4.5, 6.8, and 7.4), and selected organic solvents in tightly sealed glass vials. The samples were agitated in a shaking water bath at 25 ± 2°C for 24 h to attain equilibrium. Subsequently, the suspensions were centrifuged at 10,000 rpm for 15 min, and the supernatants were filtered through a 0.45 µm membrane filter. The concentration of dissolved cisplatin was quantified using a validated UV–Visible spectrophotometric or HPLC method. All experiments were performed in triplicate, and the results were expressed as mean ± standard deviation.[28-30]

Determination of Partition Coefficient (Log P)

The lipophilicity of cisplatin was determined using the n-octanol/water partition method. Equal volumes of n-octanol and distilled water were mutually saturated before use. Cisplatin was added to the biphasic system, followed by agitation until equilibrium was achieved. After phase separation, the drug concentration in the aqueous phase was determined using the validated analytical method. The partition coefficient (Log P) was calculated from the ratio of drug concentration in the organic phase to that in the aqueous phase.[31]

Stabilizer Screening

Pharmaceutical stabilizers, including Polyvinylpyrrolidone K30 (PVP K30), Hydroxypropyl Methylcellulose (HPMC), Poloxamer 188, and Tween 80, were screened for their ability to stabilize cisplatin nanocrystals during the precipitation process. Preliminary formulations containing different stabilizer concentrations were prepared and evaluated for particle size, polydispersity index (PDI), zeta potential, physical appearance, sedimentation behavior, and dispersion stability over 24–72 h. Based on these physicochemical characteristics, the most suitable stabilizer was selected for further optimization of the nanocrystal formulation.[32-33]

Design of Experiments (DoE) Using Box–Behnken Design

A three-factor, three-level Box–Behnken design was applied using Design-Expert® software for systematic optimization of the cisplatin nanocrystal formulation. Stabilizer concentration (X_1, 0.5–2.0% w/v), homogenization pressure (X_2, 600–1400 bar), and homogenization cycles (X_3, 5–20) were selected as the independent variables, while particle size (Y_1), PDI (Y_2), and zeta potential (Y_3) were evaluated as dependent responses. The formulation was optimized by targeting minimum particle size and PDI together with maximum absolute zeta potential to obtain a uniform and colloidally stable nanocrystal system.

API–Excipient Selection

Polyvinylpyrrolidone K30 (PVP K30), Hydroxypropyl Methylcellulose (HPMC), Poloxamer 188, and Tween 80 were evaluated as stabilizers based on their pharmaceutical compatibility, stabilizing efficiency, and safety profile. Drug–excipient compatibility was assessed by FTIR and DSC, while preliminary solubility studies were performed to select the most suitable stabilizer for nanocrystal formulation. The optimized formulation was subjected to accelerated (40 ± 2°C/75 ± 5% RH) and long-term (25 ± 2°C/60 ± 5% RH) stability studies according to ICH guidelines.[34-35]

Preparation of Cisplatin Nanocrystals

Cisplatin nanocrystals were prepared by the anti-solvent precipitation method followed by high-pressure homogenization. Briefly, 50 mg of cisplatin was dissolved in 5 mL methanol, vortexed for 1 min, and sonicated for 5 min. The drug solution was slowly injected (1 mL min^{-1}) into 100 mL of distilled water containing 0.5% (w/v) PVP K30 under magnetic stirring (1000 rpm). The resulting suspension was stirred for 10 min, followed by aging at 500 rpm for 30 min. The suspension was subsequently homogenized at 800 bar for five cycles while maintaining the temperature below 30°C. The nanocrystal dispersion was centrifuged at 10,000 × g for 10 min, re-dispersed in distilled water, and characterized for particle size, polydispersity index (PDI), zeta potential, and drug content. For solid-state studies, the optimized nanosuspension was freeze-dried using 5% (w/v) trehalose as a cryoprotectant.[36-40]

Preparation Process

Cisplatin nanocrystals were prepared using an anti-solvent precipitation technique followed by high-pressure homogenization. Briefly, cisplatin was dissolved in methanol to obtain a clear drug solution, while an aqueous stabilizer solution containing Polyvinylpyrrolidone K30 (PVP K30) was prepared separately. The drug solution was added dropwise into the anti-solvent under continuous magnetic stirring to induce rapid nucleation and nanocrystal formation. The resulting suspension was further processed by high-pressure homogenization to reduce particle size and obtain a uniform nanosuspension. The optimized formulation was subsequently characterized for particle size, polydispersity index, zeta potential, and drug content. When required, the nanosuspension was freeze-dried in the presence of a suitable cryoprotectant to obtain stable cisplatin nanocrystals for further characterization and evaluation.[41-42]

Process analytical controls and batch reproducibility

Process analytical controls were established to ensure the consistency and reproducibility of cisplatin nanocrystal formulations. Sixteen experimental batches (F1–F16) were prepared by varying the drug concentration, stabilizer composition, drug-to-stabilizer ratio, and solvent-to-anti-solvent ratio using the anti-solvent precipitation method followed by high-pressure homogenization. Critical process parameters were maintained under controlled conditions, and each batch was evaluated for particle size, polydispersity index (PDI), zeta potential, drug content, pH, and physical appearance. The optimized formulation was selected for subsequent physicochemical characterization, dissolution, and stability studies.[43-45]

Table 1: Composition of Experimental Nanocrystal Batches

Batch No.	Drug Conc. (mg)	Stabilizer System	Drug: Total Stabilizer Ratio	PVP K-30 (%)	HPMC E-15 (%)	Poloxamer 188 (%)	Tween 80 (%)	Solvent: Anti solvent (mL)
F1	50	PVP	1: 1	0.25	–	0.10	0.05	1: 10
F2	50	PVP	1: 2	0.50	–	0.10	0.05	1: 10
F3	50	HPMC	1: 1	–	0.25	0.10	0.05	1: 10
F4	50	HPMC	1: 2	–	0.50	0.10	0.05	1: 10
F5	100	PVP	1: 1	0.25	–	0.25	0.05	1: 20
F6	100	PVP	1: 2	0.5	–	0.25	0.05	1: 20

				0				
F7	100	HPMC	1:1	–	0.25	0.25	0.05	1:20
F8	100	HPMC	1:2	–	0.50	0.25	0.05	1:20
F9	150	PVP + Poloxamer	1:1	0.25	–	0.50	0.10	1:10
F10	150	PVP + Poloxamer	1:2	0.50	–	0.50	0.10	1:10
F11	150	HPMC + Poloxamer	1:1	–	0.25	0.50	0.10	1:10
F12	150	HPMC + Poloxamer	1:2	–	0.50	0.50	0.10	1:10
F13	200	Mixed stabilizers	1:1	0.50	0.25	0.75	0.10	1:20
F14	200	Mixed stabilizers	1:2	0.75	0.25	0.75	0.10	1:20
F15	200	Mixed stabilizers	1.5	.75	50		15	20
F16	200	Optimized combination	1:2	1.00	0.50	1.00	0.15	1:20

Optimization of Formulation:

The cisplatin nanocrystal formulation was optimized using a Quality by Design (QbD) approach based on a Box–Behnken Design (BBD) implemented in Design-Expert® software. Drug concentration, stabilizer concentration, homogenization pressure, and homogenization cycles were selected as independent variables, while particle size, polydispersity index (PDI), zeta potential, and drug content were evaluated as response variables. The experimental data were analyzed by ANOVA, and numerical optimization was performed using the desirability function to obtain the optimized formulation. The optimized batch was prepared in triplicate to verify the reproducibility and reliability of the optimized process.[46-47]

Characterization of Cisplatin nanocrystals[48-61]

Particle size, Polydispersity index (PDI), and Zeta potential

The average particle size, polydispersity index (PDI), and zeta potential of the cisplatin nanocrystals were determined by dynamic light scattering (DLS) using a Zetasizer (Malvern Instruments, UK). All measurements were performed at 25 ± 2°C after appropriate dilution with distilled water. Particle size and PDI were used to evaluate the size distribution, while zeta potential was measured to assess the physical stability of the nanosuspension.

Crystallinity and Thermal Analysis

The crystalline properties of cisplatin nanocrystals were analyzed using X-ray diffraction (XRD; Bruker D8 Advance, Germany). Thermal behavior and stability were evaluated using differential scanning calorimetry (DSC; TA Instruments, USA) and thermogravimetric analysis (TGA; PerkinElmer TGA 4000, USA) under controlled heating conditions.

Drug Content Determination

Drug content was determined by dissolving an accurately weighed quantity of nanocrystals in a suitable solvent and analyzing the sample using a validated HPLC (Agilent 1260, USA) or UV–Visible spectrophotometric method (Shimadzu UV-

1800, Japan). The analytical method was validated according to ICH Q2(R1) guidelines.

Entrapment Efficiency

Entrapment efficiency was determined by separating the free drug from the nanocrystals through centrifugation. The drug content in the supernatant was quantified using the validated analytical method, and the entrapment efficiency was calculated using the following equation:

$$\boldsymbol{Entrapment\ Efficiency\ (\%)} = \frac{\boldsymbol{(Total\ drug - Free\ drug)}}{\boldsymbol{Total\ Drug}} \times \mathbf{100}$$

Statistical analysis

All experiments were performed in triplicate, and the results are expressed as mean ± standard deviation (SD). Statistical analysis and optimization were performed using Design-Expert® software. The effects of formulation variables were evaluated using analysis of variance (ANOVA) and response surface methodology (RSM), with $p < 0.05$ considered statistically significant. The optimized formulation was identified using the desirability function based on the selected response variables.

RESULTS AND DISCUSSION:

Physicochemical Properties of Cisplatin

The drug exhibited low aqueous solubility (2.65 ± 0.12 mg/mL) with a pH-dependent solubility profile, showing higher solubility at pH 4.0 than at pH 7.4, confirming its poor dissolution characteristics. The high melting point (270.4 ± 0.8°C) indicated good crystallinity and thermal stability, while the drug content (99.0 ± 1.2% w/w) confirmed the high purity of the active pharmaceutical ingredient. These findings highlight the poor aqueous solubility of cisplatin and support the development of a nanocrystal formulation to improve its dissolution performance.

Preformulation Analysis

Identification and Characterization

Ultraviolet Absorption Maxima (λmax)

The UV–Visible absorption spectrum of cisplatin is presented in Figure 1. The drug exhibited a characteristic absorption maximum (λmax) at 301 nm, confirming its identity and suitability for quantitative analysis. A strong absorbance was observed in the 200–210 nm regions, while the absorbance gradually decreased at higher wavelengths with negligible absorption beyond 350 nm. Based on these observations, 301 nm was selected as the analytical wavelength for subsequent spectrophotometric studies.

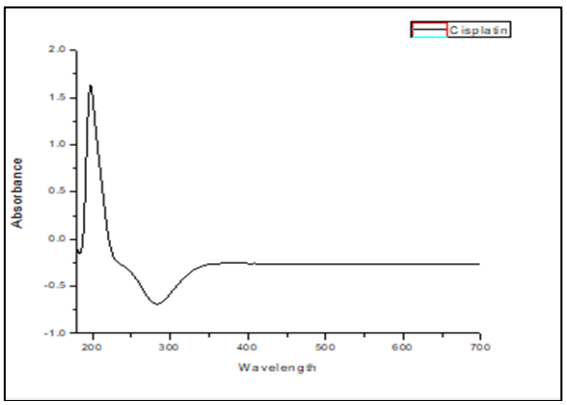

Figure 1: UV–Visible absorption spectrum of cisplatin showing the characteristic absorption maximum (λmax) at 301 nm.

Fourier Transform Infrared (FTIR) Analysis

The FTIR spectrum of pure cisplatin is shown in Figure 2. Characteristic absorption bands corresponding to N–H stretching vibrations of coordinated ammine groups were observed in the 3300–3200 cm^{-1} region, while bands at 1650–1550 cm^{-1} were attributed to N–H bending vibrations. The absorption bands below 600 cm^{-1} corresponded to Pt–N and Pt–Cl stretching vibrations, confirming the characteristic coordination structure of cisplatin. The absence of additional impurity-related peaks indicated the chemical integrity and purity of the drug.

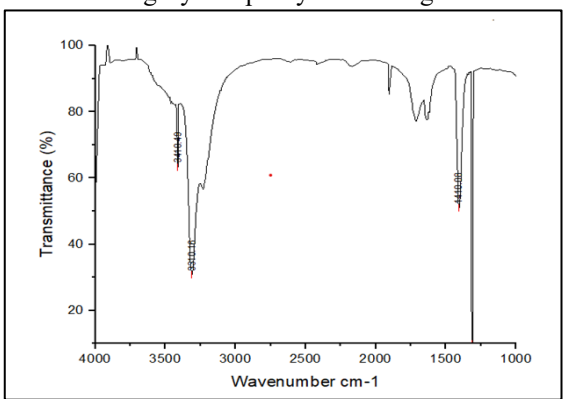

Figure 2: FTIR spectrum of pure cisplatin.

Differential Scanning Calorimetry (DSC) Analysis

The DSC thermogram of pure cisplatin is presented in Figure 3. A distinct thermal transition was observed with a sharp melting endotherm at approximately 205–210°C, indicating the crystalline nature of the drug. An exothermic transition around 134.5°C was also observed, which may be associated with structural rearrangement during heating. The sharp thermal events and absence of additional peaks confirmed the high crystallinity and thermal stability of cisplatin, supporting its suitability for nanocrystal formulation.

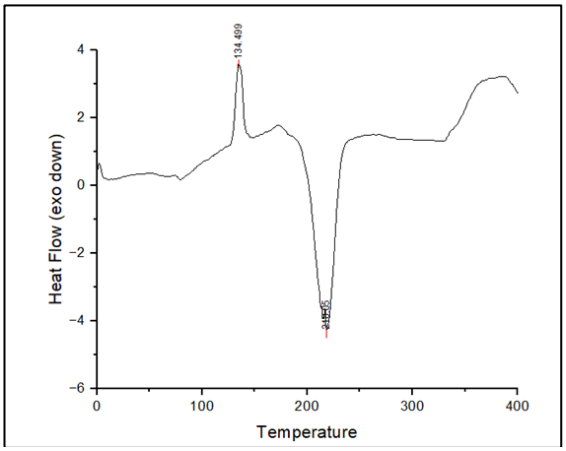

Figure 3: DSC thermogram of pure cisplatin.

Standardization of Pharmaceutical Excipients

The selected pharmaceutical excipients were evaluated according to the USP/EP pharmacopeial specifications prior to formulation development. All excipients complied with the prescribed quality requirements for physicochemical properties, including appearance, moisture content, ash content, viscosity, pH, microbial limits, and heavy metal content. The results confirmed the pharmaceutical quality and suitability of the excipients for the preparation of cisplatin nanocrystals.

Table 2: Physicochemical Evaluation of Pharmaceutical Excipients According to USP/EP Specifications

Parameter	Cerestar	Starch	Gelatin	Chitosan
Appearance	White free-flowing powder	White powder	Off-white to yellow powder	Complied
Moisture Content (%)	4.3	13.0	11.0	5.5
pH	4.5	—	—	—
Ash/Sulphated Ash (%)	0.18 / 0.095	0.50	1.80	0.95
Viscosity	290 mPas	—	—	200 cps
Heavy Metals	4 mg/kg	—	5 ppm	—
Microbial Limits	Absent	Absent	Complied	Complied
Overall Compliance	USP/EP	USP/EP	USP/EP	USP/EP

The physicochemical evaluation demonstrated that all excipients met the pharmacopoeial acceptance criteria and were suitable for nanocrystal formulation. Their compliance with USP/EP specifications ensured adequate purity, stability, and compatibility, supporting their application in the Quality by Design (QbD)-based development of cisplatin nanocrystals.

Solubility Studies

Cisplatin exhibited slight solubility in purified water (~1.0 mg/mL) and was practically insoluble in ethanol (<0.1 mg/mL). In contrast, the drug showed markedly higher solubility in DMF (10–20 mg/mL) and DMSO (20–50 mg/mL). These findings confirm the poor aqueous solubility of cisplatin and support the application of nanocrystal technology to enhance its dissolution behavior and pharmaceutical performance.

Partition Coefficient

Negative log P values were observed in all solvent systems, indicating the hydrophilic nature of cisplatin. The lowest value was obtained in n-octanol/PBS (−2.25 ± 0.02), while the highest value was recorded in n-octanol/DMSO (−0.76 ± 0.06). The low partition coefficient confirms the poor membrane permeability of cisplatin and further justifies the development of nanocrystal formulations to improve its biopharmaceutical performance.

Standard Calibration Curves of Cisplatin

Standard calibration curves of cisplatin were established in different dissolution media to evaluate the linearity and applicability of the analytical method. Excellent linear relationships between drug concentration and absorbance were obtained in all media, confirming compliance with Beer–Lambert's law. The calibration curves showed high correlation coefficients (R^2 = 0.9977–0.9992), indicating good linearity, accuracy, and reproducibility over the selected concentration ranges. Among the tested media, the highest analytical sensitivity was observed in phosphate buffer (pH 7.4) and dimethylformamide (DMF), while the OPD colorimetric method demonstrated improved absorbance with increasing reagent concentration and reaction time. These findings confirmed the suitability of the developed analytical method for the quantitative estimation of cisplatin during formulation and dissolution studies.

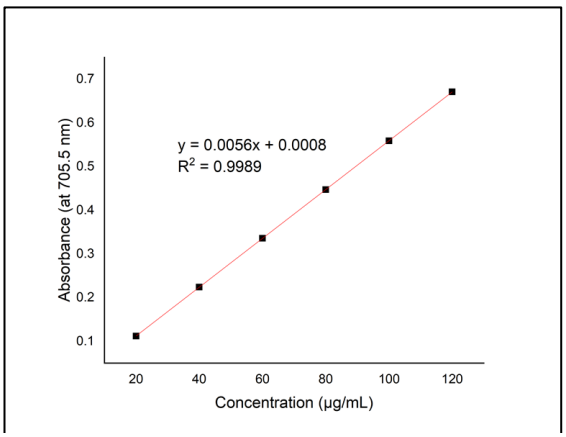

Figure 4: Calibration curve of cisplatin in phosphate buffer (pH 6.8).

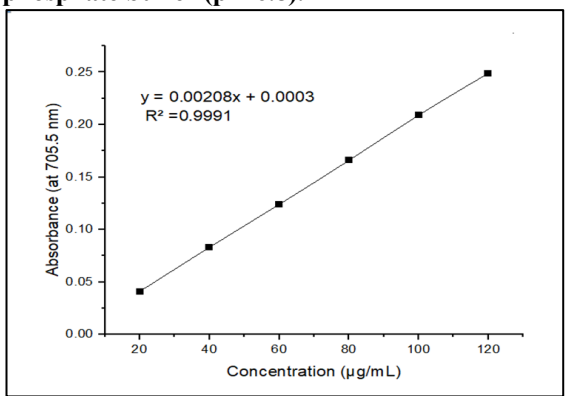

Figure 5: Calibration curve of cisplatin in buffer (pH 1.2).

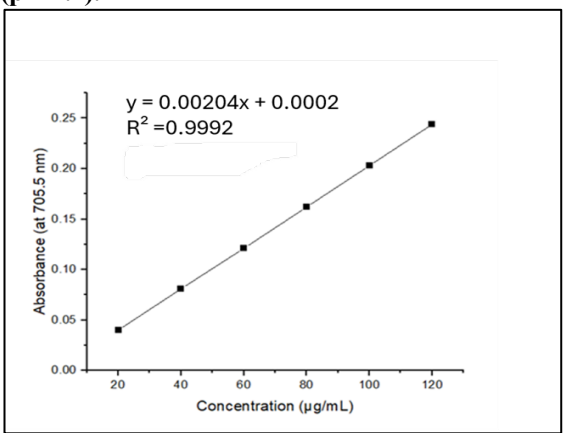

Figure 6: Calibration curve of cisplatin in buffer (pH 4.5).

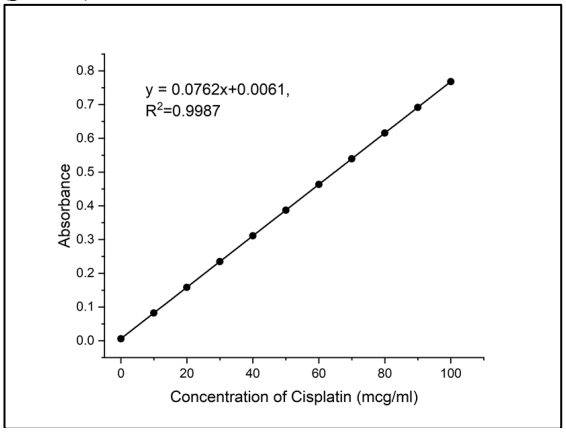

Figure 7: Calibration curve of cisplatin in phosphate buffer (pH 7.4).

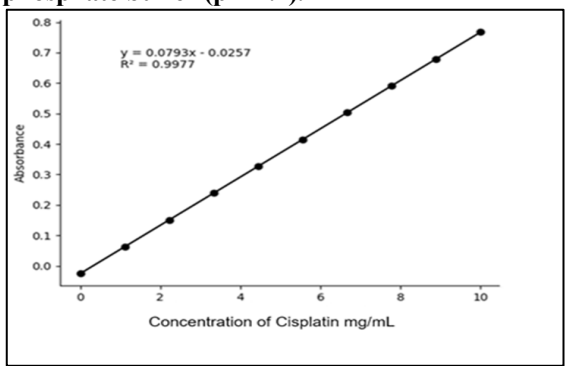

Figure 8: Calibration curve of cisplatin in dimethylformamide (DMF).

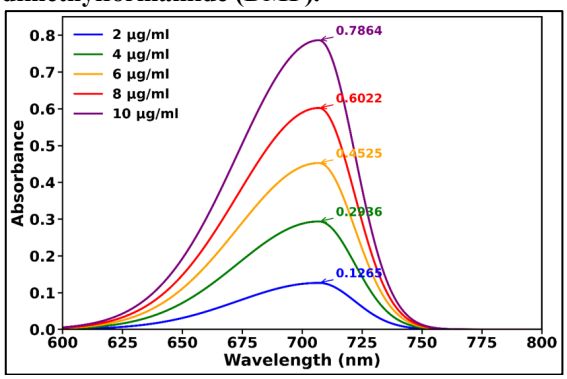

Figure 9: Effect of OPD concentration on cisplatin complex formation.

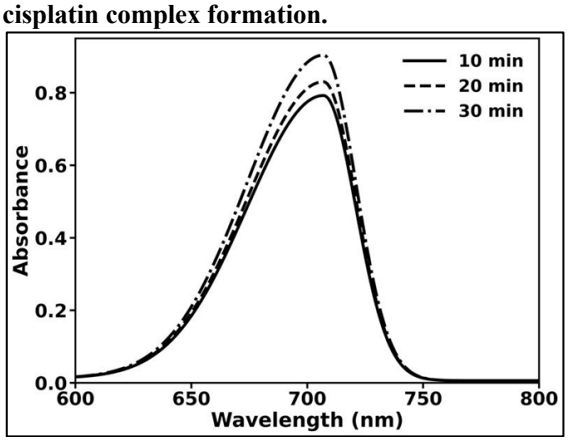

Figure 10: Effect of reaction time on cisplatin–OPD complex formation.

Nanocrystal Preparation and Optimization

Nanocrystals were optimized using a Quality by Design (QbD) approach by evaluating the effects of stabilizer concentration, homogenization pressure, and homogenization cycles on the critical quality attributes. The response surface analysis demonstrated that increasing stabilizer concentration and homogenization pressure significantly reduced particle size, while additional homogenization cycles further improved particle size reduction and uniformity. A decrease in the polydispersity index (PDI) indicated a narrower particle size distribution, whereas higher stabilizer concentrations produced more negative zeta potential values, suggesting improved colloidal

stability and reduced particle aggregation. Overall, the optimized processing conditions resulted in nanocrystals with desirable particle size, uniform distribution, and enhanced physical stability.

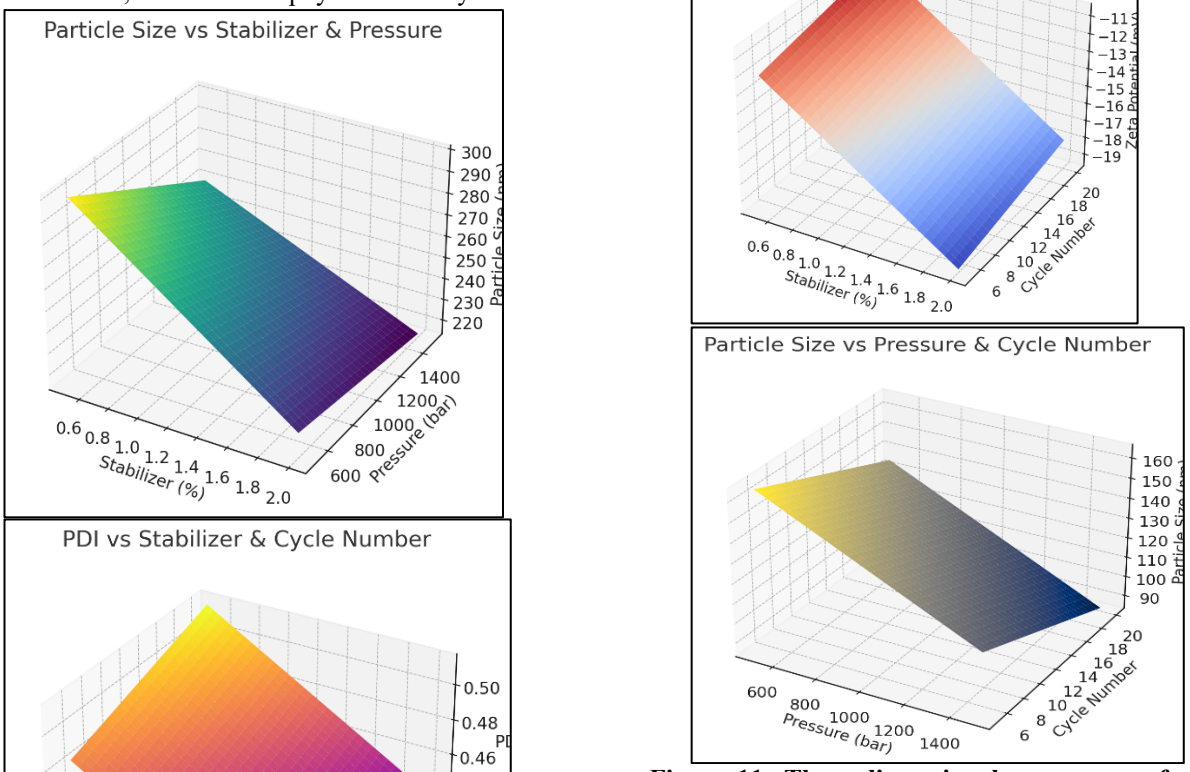

Figure 11: Three-dimensional response surface plots illustrating the effects of stabilizer concentration, homogenization pressure, and homogenization cycles on (a) particle size, (b) polydispersity index (PDI), (c) zeta potential, and (d) particle size during nanocrystal optimization.

Characterization of Prepared Nanocrystals

Particle Size, Polydispersity Index (PDI), and Zeta Potential

The particle size analysis demonstrated a significant reduction in particle size following nanocrystal formulation (Table 3). Pure cisplatin exhibited a larger average particle size (~1950 nm) with a broad size distribution (PDI = 0.58), whereas the optimized nanocrystals showed a mean particle size of approximately 160 nm with a substantially lower PDI (0.21), indicating a narrow and uniform particle size distribution. Furthermore, the nanocrystals exhibited a zeta potential of −45 to −50 mV, suggesting excellent colloidal stability and reduced aggregation. These findings confirmed the successful preparation of stable cisplatin nanocrystals with improved physicochemical characteristics.

Table 3: Particle Size Characteristics of Pure Cisplatin and Optimized Nanocrystals

Parameter	Pure Cisplatin	Cisplatin Nanocrystals
d10 (nm)	~1350	~80

d50 (nm)	~1850	~150
d90 (nm)	~2650	~250
Mean Particle Size (nm)	~1950	~160
Polydispersity Index (PDI)	0.58	0.21
Zeta Potential (mV)	Not determined	−45 to −50

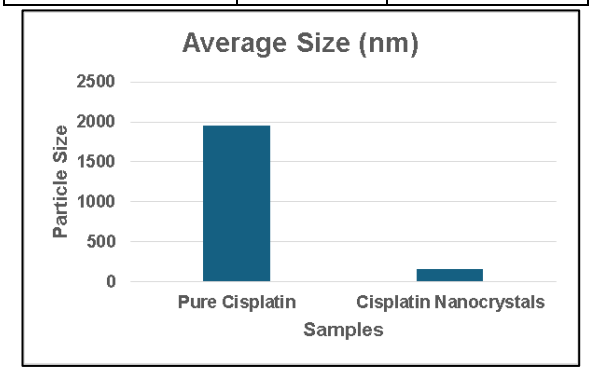

Figure 12: Particle size distribution of pure Cisplatin and optimized nanocrystals.

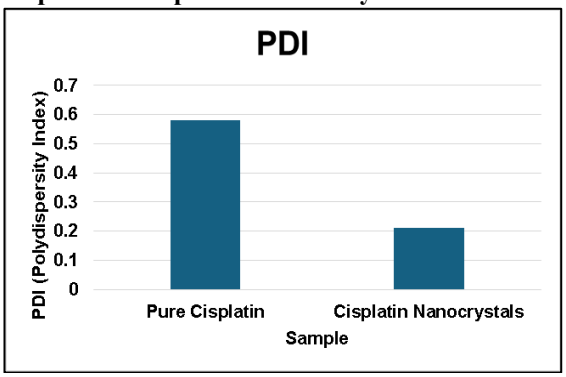

Figure 13: Comparison of the polydispersity index (PDI) of pure Cisplatin and nanocrystals.

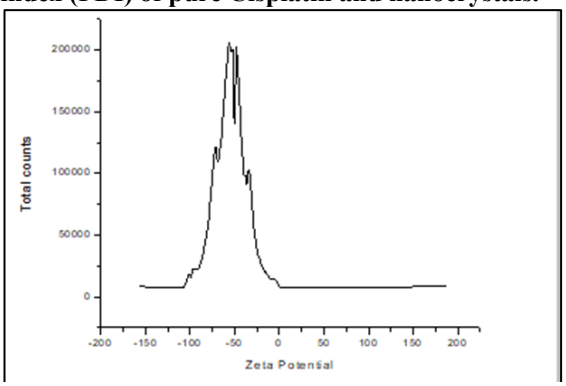

Figure 14: Zeta potential distribution of optimized Cisplatin nanocrystals.

Crystallinity and Thermal Behaviour

X-ray Diffraction (XRD) Analysis

The XRD patterns of pure cisplatin and its nanocrystals demonstrated a noticeable reduction in peak intensity and crystallinity following nanosizing. Pure cisplatin exhibited characteristic sharp diffraction peaks, whereas the nanocrystals showed broader and less intense peaks, indicating partial loss of crystallinity, which is expected to improve the dissolution characteristics of the drug.

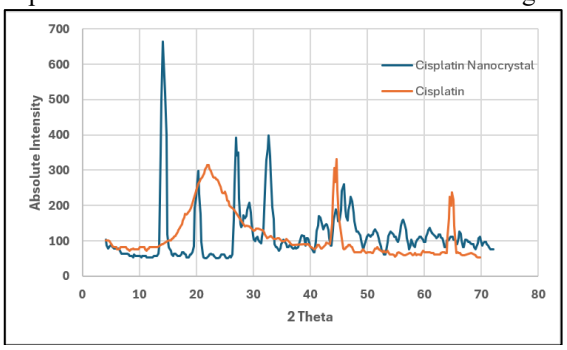

Figure 15: X-ray diffraction (XRD) patterns of pure cisplatin and optimized cisplatin nanocrystals.

Differential Scanning Calorimetry (DSC) Analysis

The DSC thermograms showed a distinct melting endotherm for pure cisplatin, confirming its crystalline nature. The optimized nanocrystals exhibited a broader and less intense endothermic peak with a slight shift toward a lower temperature, indicating reduced crystallinity and partial amorphization after nanosization while maintaining adequate thermal stability.

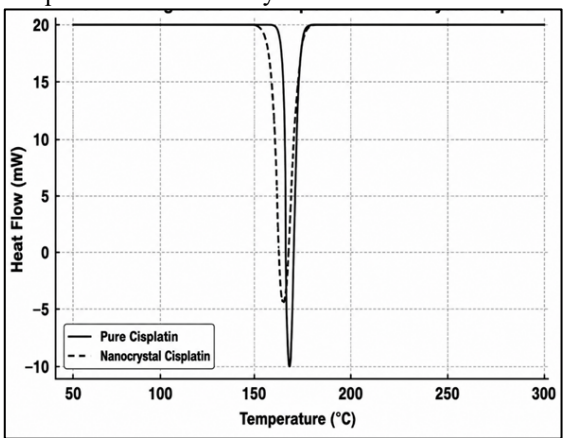

Figure 16: Differential scanning calorimetry (DSC) thermograms of pure Cisplatin and optimized cisplatin nanocrystals.

Thermogravimetric Analysis (TGA)

Thermogravimetric analysis demonstrated that both pure cisplatin and the optimized nanocrystals remained thermally stable up to approximately 250°C, followed by thermal degradation at higher temperatures. The nanocrystals exhibited a slightly lower degradation onset temperature than the pure drug, which may be attributed to the increased surface area following particle size reduction. Overall, both formulations showed satisfactory thermal stability for pharmaceutical processing.

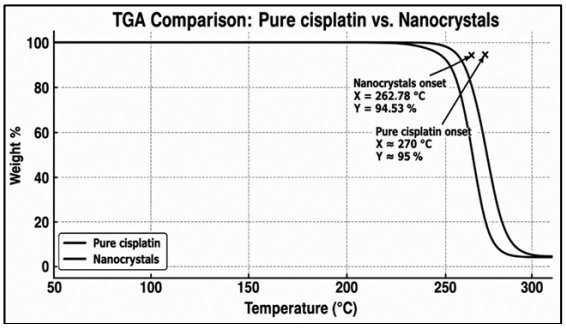

Figure 17: Thermogravimetric analysis (TGA) of pure cisplatin and optimized cisplatin nanocrystals.

Drug Content and Encapsulation Efficiency

The optimized cisplatin nanocrystals exhibited a drug content of 98.2 ± 1.1% and an encapsulation efficiency of 89.7 ± 1.4%, indicating efficient drug incorporation with minimal drug loss during formulation. These results demonstrate the effectiveness of the developed nanocrystal formulation and confirm the reliability of the HPLC method for quantitative drug estimation.

Table 4: Drug Content and Encapsulation Efficiency of Optimized Cisplatin Nanocrystals

Parameter	Value (Mean ± SD)
Drug Content (%)	98.2 ± 1.1
Encapsulation Efficiency (%)	89.7 ± 1.4

HPLC Analysis of Pure Cisplatin

The HPLC chromatogram of pure cisplatin showed a sharp and symmetrical peak at a retention time of 4.2347 min with detection at 310 nm, confirming the identity and purity of the drug without interference from impurities or degradation products.

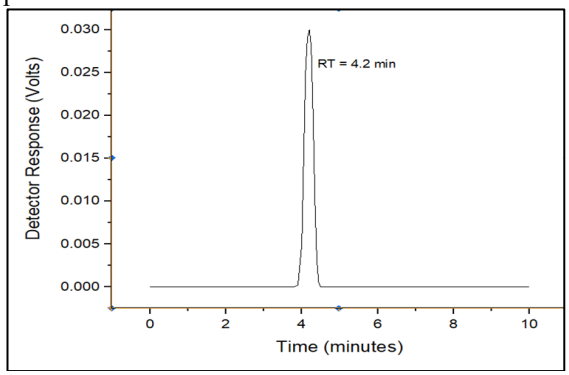

Figure 18: HPLC chromatogram of pure cisplatin showing a characteristic peak at a retention time of 4.2347 min detected at 310 nm.

HPLC Analysis of Optimized Cisplatin Nanocrystals

The HPLC chromatogram of the optimized cisplatin nanocrystals exhibited a well-defined peak at the same retention time (4.2347 min) as the pure drug, confirming successful drug incorporation without chromatographic interference from formulation excipients.

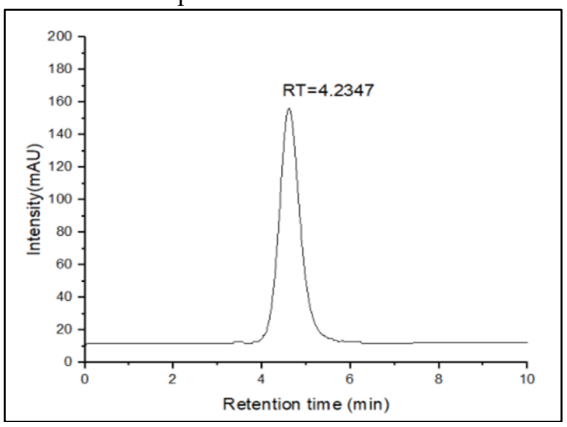

Figure 19: HPLC chromatogram of optimized cisplatin nanocrystals showing a characteristic drug peak at a retention time of 4.2347 min detected at 310 nm.

CONCLUSION:

The present study successfully developed and optimized cisplatin nanocrystals using a Quality by Design (QbD) approach combined with anti-solvent precipitation and high-pressure homogenization. Preformulation studies confirmed the poor aqueous solubility and low permeability of cisplatin, supporting the need for a nanocrystal-based formulation strategy. Optimization using the Box–Behnken Design identified the critical formulation and process variables influencing particle size, polydispersity index, zeta potential, and drug content. The optimized nanocrystal formulation demonstrated a marked reduction in particle size with a narrow size distribution and excellent colloidal stability. Solid-state characterization by XRD, DSC, and TGA confirmed reduced crystallinity while maintaining adequate thermal stability. The formulation also exhibited high drug content and encapsulation efficiency, indicating efficient drug incorporation with minimal processing loss. The validated analytical method further confirmed reliable and reproducible quantification of cisplatin. Overall, the developed nanocrystal formulation provides a robust and reproducible platform for improving the physicochemical characteristics of cisplatin. The enhanced particle characteristics achieved through QbD-driven optimization are expected to contribute to improved dissolution behavior and pharmaceutical performance. These findings support the potential application of nanocrystal technology for the delivery of poorly soluble BCS Class IV anticancer drugs and provide a strong basis for subsequent in vitro dissolution, permeability, and anticancer evaluation.

CONFLICT OF INTEREST:

The authors declare that there are no conflicts of interest.

REFERENCES:

1. Zang W, Gao D, Yu M, Long M, Zhang Z, Ji T. Oral delivery of gemcitabine-loaded glycocholic acid-modified micelles for cancer therapy. ACS Nano. 2023;17(18):18074-18088. doi:10.1021/acsnano.3c04953.
2. Freeman MW. Toward the patient-centered development of cancer therapeutics: a focus on nanomedicines [dissertation]. Toronto (ON): University of Toronto; 2018.
3. Guan ZZ, Li QL, Feng F, Jiang Z, Shen Z, Yu S, et al. Superior efficacy of a Cremophor-free albumin-bound paclitaxel compared with solvent-based paclitaxel in Chinese patients with metastatic breast cancer. Asia Pac J Clin Oncol. 2009;5(3):165-174. doi:10.1111/j.1743-7563.2009.01199.x.
4. Postel-Vinay S, Collette L, Paoletti X, Rizzo E, Massard C, Olmos D, et al. Towards new methods for the determination of dose-limiting toxicities and the assessment of the recommended dose for further studies of molecularly targeted agents: Dose-Limiting Toxicity and Toxicity Assessment Recommendation Group for Early Trials of Targeted Therapies, an European Organisation for Research and Treatment of Cancer-led study. Eur J Cancer. 2014;50(12):2040-2049. doi:10.1016/j.ejca.2014.04.009.
5. Joerger M. Metabolism of the taxanes including nab-paclitaxel. Expert Opin Drug Metab Toxicol. 2015;11(5):691-702. doi:10.1517/17425255.2015.1021681.
6. Ventola CL. Progress in nanomedicine: approved and investigational nanodrugs. PT. 2017;42(12):742-755.
7. Soria JC, Massard C, Le Chevalier T. Should progression-free survival be the primary measure of efficacy for advanced NSCLC therapy? Ann Oncol. 2010;21(12):2324-2332. doi:10.1093/annonc/mdq175.
8. Melo MN, Amaral RG, Melo de Andrade LR, Severino P, Blanco-Llamero C, Andrade LN, et al. A review of randomized phase III clinical trials of cancer nanomedicines. Cancer Pathog Ther. 2024;2:E01-E15. doi:10.36922/cpt.3755.
9. Khan MI, Hossain MI, Hossain MK, Rubel MH, Hossain KM, Mahfuz AM, et al. Recent progress in nanostructured smart drug delivery systems for cancer therapy: a review. ACS Appl Bio Mater. 2022;5(3):971-1012. doi:10.1021/acsabm.1c01231.
10. Batchelor HK, Fotaki N, Klein S. Paediatric oral biopharmaceutics: key considerations and current challenges. Adv Drug Deliv Rev. 2014;73:102-126. doi:10.1016/j.addr.2013.10.006.
11. Manshi, Setya S, Talegaonkar S. Advances and developments in formulation of drug nanocrystals. In: Advances in Pharmaceutical Product Development. Singapore: Springer Nature; 2025. p.321-354.
12. Lee MK. Liposomes for enhanced bioavailability of water-insoluble drugs: in vivo evidence and recent approaches. Pharmaceutics. 2020;12(3):264. doi:10.3390/pharmaceutics12030264.
    Niu G, Ruditskiy A, Vara M, Xia Y. Toward continuous and scalable production of colloidal nanocrystals by switching from batch to droplet reactors. Chem Soc Rev. 2015;44(16):5806-5820. doi:10.1039/C5CS00183A.
13. Thakkar S, Shah V, Misra M, Kalia K. Nanocrystal-based drug delivery system: conventional and current scenario. Recent Pat Nanotechnol. 2017;11(2):130-145. doi:10.2174/1872210511666170201154835.
14. Gaspar R, Duncan R. Polymeric carriers: preclinical safety and the regulatory implications for design and development of polymer therapeutics. Adv Drug Deliv Rev. 2009;61(13):1220-1231. doi:10.1016/j.addr.2009.06.003.
    Kasiński A, Zielińska-Pisklak M, Oledzka E, Sobczak M. Smart hydrogels: synthetic stimuli-responsive antitumor drug release systems. Int J Nanomedicine. 2020;15:4541-4572. doi:10.2147/IJN.S243012.
15. Meli V, Caltagirone C, Falchi AM, Hyde ST, Lippolis V, Monduzzi M, et al. Docetaxel-loaded fluorescent liquid-crystalline nanoparticles for cancer theranostics. Langmuir. 2015;31(35):9566-9575. doi:10.1021/acs.langmuir.5b01920.
16. Jacob J, Haponiuk JT, Thomas S, Gopi S. Biopolymer-based nanomaterials in drug delivery systems. Mater Today Chem. 2018;9:43-55. doi:10.1016/j.mtchem.2018.05.003.
    Wang Z, Wang X, Xu W, Li Y, Lai R, Qiu X, et al. Translational challenges and prospective solutions in the implementation of biomimetic delivery systems. Pharmaceutics. 2023;15(11):2623. doi:10.3390/pharmaceutics15112623.
17. Peltonen L, Strachan C. Understanding critical quality attributes for nanocrystals from preparation to delivery. Molecules. 2015;20(12):22286-22300. doi:10.3390/molecules201219847.
18. Farkas N, Kramar JA. Dynamic light scattering distributions by any means. J Nanopart Res. 2021;23(5):120. doi:10.1007/s11051-021-05236-7.
19. Bhalani DV, Nutan B, Kumar A, Chandel AKS. Bioavailability enhancement techniques for poorly aqueous soluble drugs and therapeutics. Biomedicines. 2022;10(9):2055. doi:10.3390/biomedicines10092055.

20. Falsafi SR, Rostamabadi H, Assadpour E, Jafari SM. Morphology and microstructural analysis of bioactive-loaded micro/nanocarriers via microscopy techniques: CLSM, SEM, TEM and AFM. Adv Colloid Interface Sci. 2020;280:102166. doi:10.1016/j.cis.2020.102166.
21. Chircov C, Petcu MC, Vasile BS, Purcăreanu B, Nicoară AI, Oprea OC, et al. Irinotecan-loaded magnetite-silica core-shell systems for colorectal cancer treatment. Int J Pharm. 2024;661:124420. doi:10.1016/j.ijpharm.2024.124420.
22. Gil-González E, Perejón A, Sánchez-Jiménez PE, Medina-Carrasco S, Kupčík J, Šubrt J, et al. Crystallization kinetics of nanocrystalline materials by combined X-ray diffraction and differential scanning calorimetry experiments. Cryst Growth Des. 2018;18(5):3107-3116. doi:10.1021/acs.cgd.8b00120.
23. Cheng M, Liu Q, Gan T, Fang Y, Yue P, Sun Y, et al. Nanocrystal-loaded micelles for the enhanced in vivo circulation of docetaxel. Molecules. 2021;26(15):4481. doi:10.3390/molecules26154481.
24. Jiang J, Oberdörster G, Biswas P. Characterization of size, surface charge, and agglomeration state of nanoparticle dispersions for toxicological studies. J Nanopart Res. 2009;11(1):77-89. doi:10.1007/s11051-008-9446-4.
25. Liang H, Zou F, Liu Q, Wang B, Fu L, Liang X, et al. Nanocrystal-loaded liposome for targeted delivery of poorly water-soluble antitumor drugs with high drug loading and stability towards efficient cancer therapy. Int J Pharm. 2021;599:120418. doi:10.1016/j.ijpharm.2021.120418.
26. Zuccari G, Baldassari S, Ailuno G, Turrini F, Alfei S, Caviglioli G. Formulation strategies to improve oral bioavailability of ellagic acid. Appl Sci. 2020;10(10):3353. doi:10.3390/app10103353.
27. Chary SS, Bhikshapathi DV, Vamsi NM, Kumar JP. Optimizing entrectinib nanosuspension: Quality by Design for enhanced oral bioavailability and minimized fast-fed variability. BioNanoScience. 2024;14(4):4551-4569. doi:10.1007/s12668-024-01574-7.
28. Fendler JH, editor. Nanoparticles and nanostructured films: preparation, characterization, and applications. Hoboken (NJ): John Wiley & Sons; 2008.
29. Rahdar A, Amini N, Askari F, Susan MABH. Dynamic light scattering: a useful technique to characterize nanoparticles. J Nanoanalysis. 2019;6(2):80-93.
30. Wei L, Ji Y, Gong W, Kang Z, Meng M, Zheng A, et al. Preparation, physical characterization and pharmacokinetic study of paclitaxel nanocrystals. Drug Dev Ind Pharm. 2015;41(8):1343-1352. doi:10.3109/03639045.2014.956046.
31. Kohli K, Mujtaba A, Malik R, Amin S, Alam MS, Ali A, et al. Development of natural polysaccharide-based nanoparticles of berberine to enhance oral bioavailability: formulation, optimization, ex vivo, and in vivo assessment. Polymers (Basel). 2021;13(21):3833. doi:10.3390/polym13213833.
32. Gupta P, Rai N, Verma A, Gautam V. Microscopy-based methods for characterization, drug delivery, and understanding the dynamics of nanoparticles. Med Res Rev. 2024;44(1):138-168. doi:10.1002/med.21992.
33. Mahmoud BS, McConville C. Development and optimization of irinotecan-loaded PCL nanoparticles and their cytotoxicity against primary high-grade glioma cells. Pharmaceutics. 2021;13(4):541. doi:10.3390/pharmaceutics13040541.
34. Thakkar S, Misra M. Electrospray drying of docetaxel nanosuspension: a study on particle formation and evaluation of nanocrystals thereof. J Drug Deliv Sci Technol. 2020;60:102009. doi:10.1016/j.jddst.2020.102009.
35. Pardhi VP, Verma T, Flora SJS, Chandasana H, Shukla R. Nanocrystals: an overview of fabrication, characterization and therapeutic applications in drug delivery. Curr Pharm Des. 2018;24(43):5129-5146. doi:10.2174/1381612825666190116151407.
36. Mills JA, Liu F, Jarrett TR, Fletcher NL, Thurecht KJ. Nanoparticle-based medicines: approaches for evading and manipulating the mononuclear phagocyte system and potential for clinical translation. Biomater Sci. 2022;10(12):3029-3053. doi:10.1039/D1BM01931G.
37. Guo M, Qin S, Wang S, Sun M, Yang H, Wang X, et al. Herbal medicine nanocrystals: a potential novel therapeutic strategy. Molecules. 2023;28(17):6370. doi:10.3390/molecules28176370.
38. Bates S, Zografi G, Engers D, Morris K, Crowley K, Newman A. Analysis of amorphous and nanocrystalline solids from their X-ray diffraction patterns. Pharm Res. 2006;23(10):2333-2349. doi:10.1007/s11095-006-9084-4.
39. Thakral S, Terban MW, Thakral NK, Suryanarayanan R. Recent advances in the characterization of amorphous pharmaceuticals by X-ray diffractometry. Adv Drug Deliv Rev. 2016;100:183-193. doi:10.1016/j.addr.2016.01.005.

40. Bhattacharya S, Sharma S, Prajapati BG. Development of D-α-tocopherol polyethylene glycol 1000 succinate fabricated nanostructured lipid carrier of sorafenib tosylate for metastatic colorectal targeting application: stability, physical characterization, cytotoxicity, and apoptotic studies against SW48 cells PTEN. Front Oncol. 2022;12:990841. doi:10.3389/fonc.2022.990841.
41. Leyva-Porras C, Cruz-Alcantar P, Espinosa-Solís V, Martínez-Guerra E, Piñón-Balderrama CI, Compeán-Martínez I, et al. Application of differential scanning calorimetry (DSC) and modulated differential scanning calorimetry (MDSC) in food and drug industries. Polymers (Basel). 2020;12(1):5. doi:10.3390/polym12010005.
42. Swarnakar NK, Thanki K, Jain S. Bicontinuous cubic liquid crystalline nanoparticles for oral delivery of doxorubicin: implications on bioavailability, therapeutic efficacy, and cardiotoxicity. Pharm Res. 2014;31(5):1219-1238. doi:10.1007/s11095-013-1248-4.
43. Zhang F, Long XT, Ren BY, Dai XL, Lu TB, Chen JM. Three polymorphs and two hydrates of a multidrug crystal involving gefitinib and rhein: characterization, stability, and solubility aspects. Cryst Growth Des. 2024;24(11):4501-4509. doi:10.1021/acs.cgd.4c00255.
Fakayode SO, Baker GA, Bwambok DK, Bhawawet N, Elzey B, Siraj N, et al. Molecular (Raman, NIR, and FTIR) spectroscopy and multivariate analysis in consumable products analysis. Appl Spectrosc Rev. 2020;55(8):647-723. doi:10.1080/05704928.2019.1677610.
44. Bonaccorso A, Gigliobianco MR, Pellitteri R, Santonocito D, Carbone C, Di Martino P, et al. Optimization of curcumin nanocrystals as a promising strategy for nose-to-brain delivery application. Pharmaceutics. 2020;12(5):476. doi:10.3390/pharmaceutics12050476.
45. Ashin ZF, Sadeghi-Mohammadi S, Vaezi Z, Najafi F, AdibAmini S, Sadeghizadeh M, et al. Synergistic effect of curcumin and tamoxifen loaded in pH-responsive gemini surfactant nanoparticles on breast cancer cells. BMC Complement Med Ther. 2024;24(1):337. doi:10.1186/s12906-024-04665-0.
46. Kumar M, Goswami P, Jha A, Manjit M, Satpute AP, Koch B, et al. Formulation and evaluation of cetuximab-functionalized phospholipid-modified nanocrystals of paclitaxel for non-small cell lung cancer therapy. Sci Rep. 2024;14(1):29114. doi:10.1038/s41598-024-80364-5.
47. Gupta R, Chen Y, Xie H. In vitro dissolution considerations associated with nano drug delivery systems. WIREs Nanomed Nanobiotechnol. 2021;13(6):e1732. doi:10.1002/wnan.1732.
48. Chowdhury P. Novel paclitaxel nanoparticles for enhanced therapeutic effects in breast cancer [dissertation]. Memphis (TN): The University of Tennessee Health Science Center; 2020.
49. Gopakumar L, Sreeranganathan M, Chappan S, James S, Gowd GS, Manohar M, et al. Enhanced oral bioavailability and antitumor therapeutic efficacy of sorafenib administered in core-shell protein nanoparticle. Drug Deliv Transl Res. 2022;12(11):2824-2837. doi:10.1007/s13346-022-01170-6.
50. Midekessa G, Godakumara K, Ord J, Viil J, Lättekivi F, Dissanayake K, et al. Zeta potential of extracellular vesicles: toward understanding the attributes that determine colloidal stability. ACS Omega. 2020;5(27):16701-16710. doi:10.1021/acsomega.0c02057.
51. Ma WF, Wu KY, Tang J, Li D, Wei C, Guo J, et al. Magnetic drug carrier with a smart pH-responsive polymer network shell for controlled delivery of doxorubicin. J Mater Chem. 2012;22(30):15206-15214. doi:10.1039/C2JM32087A.
52. 160. Khani O, Mohammadi M, Khaz'ali AR, Aghdam MA. Effect of pH value and zeta potential on the stability of CO_2 foam stabilized by SDS surfactant and SiO_2, ZnO and Fe_2O_3 nanoparticles. Sci Rep. 2025;15(1):10302. doi:10.1038/s41598-025-10302-0.
53. Muthu MS, Feng SS. Pharmaceutical stability aspects of nanomedicines. Nanomedicine (Lond). 2009;4(8):857-860. doi:10.2217/nnm.09.74.
54. Sayyad P, Jha S, Sharma R, Yadav V, Jain S. Unveiling the potential of nanosuspension formulation strategy for improved oral bioavailability of gefitinib. AAPS PharmSciTech. 2025;26(2):59. doi:10.1208/s12249-024-03178-3.
55. Zheng B, McClements DJ. Formulation of more efficacious curcumin delivery systems using colloid science: enhanced solubility, stability, and bioavailability. Molecules. 2020;25(12):2791. doi:10.3390/molecules25122791.
56. Aungst BJ. Optimizing oral bioavailability in drug discovery: an overview of design and testing strategies and formulation options. J Pharm Sci. 2017;106(4):921-929. doi:10.1016/j.xphs.2016.12.008.
57. Sood R, Tomar D, Kaushik P, Sharma P, Rani N, Guarve K, et al. Enhanced solubility and increased bioavailability with engineered nanocrystals. Curr Drug Ther. 2024;19(6):638-

647. doi:10.2174/1574885519666240226101655.
58. Agrahari V, Agrahari V. Facilitating the translation of nanomedicines to a clinical product: challenges and opportunities. Drug Discov Today. 2018;23(5):974-991. doi:10.1016/j.drudis.2018.01.014.
59. Veronica N, Heng PWS, Liew CV. Ensuring product stability: choosing the right excipients. J Pharm Sci. 2022;111(8):2158-2171. doi:10.1016/j.xphs.2022.03.018.
60. Ribeiro A, Montes F, Sousa J, Pais A. Comminution technologies in the pharmaceutical industry: a comprehensive review with recent advances. Rev Chem Eng. 2025;41(1):69-100. doi:10.1515/revce-2023-0124.
61. Pingale P, Kendre P, Pardeshi K, Rajput A. An emerging era in manufacturing of drug delivery systems: nanofabrication techniques. Heliyon. 2023;9(3):e14061. doi:10.1016/j.heliyon.2023.e14061.